







Effects of loose deposits on debris flow processes in the Aizi Valley, southwest China


LIU Mei^{1,2}  <https://orcid.org/0000-0001-8121-5772>; e-mail: lmeimei90@163.com

ZHANG Yong^{1,2}  <https://orcid.org/0000-0002-2860-985X>; e-mail: zhangyongcas@163.com

TIAN Shu-feng^{1,2}  <https://orcid.org/0000-0002-9385-0746>; e-mail: 05131895@cumt.edu.cn

CHEN Ning-sheng^{1*}  <https://orcid.org/0000-0002-6135-0739>;  e-mail: chennsh@imde.ac.cn

MAHFUZR Rahman^{1,3}  <https://orcid.org/0000-0001-8402-156X>; e-mail: mfz.rahman@iubat.edu

JAVED Iqbal^{1,4}  <https://orcid.org/0000-0001-5409-2607>; e-mail: javediqbalgeo@gmail.com

* Corresponding author

¹ Key Lab of Mountain Hazards and Surface Processes, Institute of Mountain Hazards and Environment, Chinese Academy of Sciences, Chengdu 610041, China.

² University of Chinese Academy of Sciences, Beijing 100049, China

³ Department of Civil Engineering, International University of Business Agriculture and Technology, Dhaka 1230, Bangladesh

⁴ Department of geology, The university of Haripur, Haripur 22620, Pakistan

Citation: Liu M, Zhang Y, Tian SF, et al. (2020) Effects of loose deposits on debris flow processes in the Aizi Valley, southwest China. *Journal of Mountain Science* 17(1). <https://doi.org/10.1007/s11629-019-5388-9>

© Science Press, Institute of Mountain Hazards and Environment, CAS and Springer-Verlag GmbH Germany, part of Springer Nature 2020

Abstract: Loose deposits, rainfall and topography are three key factors that triggering debris flows. However, few studies have investigated the effects of loose deposits on the whole debris flow process. On June 28, 2012, a catastrophic debris flow occurred in the Aizi Valley, resulting in 40 deaths. The Aizi Valley is located in the Lower Jinsha River, southwestern Sichuan Province, China. The Aizi Valley debris flow has been selected as a case for addressing loose deposits effects on the whole debris flow process through remote sensing, field investigation and field experiments. Remote sensing interpretation and laboratory experiments were used to obtain the distribution and characteristics of the loose deposits, respectively. A field experiment was conducted to explore the

mechanics of slope debris flows, and another field investigation was conducted to obtain the processes of debris flow formation, movement and amplification. The results showed that loose deposits preparation, slope debris flow initiation, gully debris flow confluence and valley debris flow amplification were dominated by the loose deposits. Antecedent droughts and earthquake activities may have increased the potential for loose soil sources in the Aizi Valley, which laid the foundation for debris flow formation. Slope debris flow initiated under rainfall, and the increase in the water content as well as the pore water pressure of the loose deposits were the key factors affecting slope failure. The nine gully debris flows converged in the valley, and the peak discharge was amplified 3.3 times due to a blockage and outburst caused by a large boulder. The results may help in predicting and assessing regional debris flows in dry-hot and seismic-prone areas based on

Received: 14-Jan-2019
1st Revision: 21-Mar-2019
2nd Revision: 27-Oct-2019
Accepted: 27-Nov-2019

loose deposits, especially considering large boulders.

Keywords: Aizi Valley; Loose deposits; Debris flow process; Slope debris flow; Boulder blockage; Discharge amplification

Introduction

Debris flows are distinct floods of solid materials such as mud, sand and boulders that originate from high, steep slopes or channels during precipitation (Iverson et al. 1997). The loose deposits, water and topography are the three basic elements required for debris flow formation. Generally, watershed height differences of more than 300 m, channel slopes of more than 15°, and rainfall amounts of over 9 mm per hour can trigger a debris flow (Tang et al. 2009; Chen et al. 2011; Zhou and Tang 2014). Therefore, the topography and rainfall conditions in most mountainous regions can easily satisfy the debris flow formation threshold. In China, debris flows are concentrated in the southwest, especially in the dry-hot valley and seismic belt (Chen et al. 2014), and this characteristic is difficult to explain considering the accepted role of rainfall in controlling debris flow formation. Seismic belts are located in active fault zones, where large numbers of weak structures and broken rocks are developed along the fracture zone (Pareek et al. 2010; Guo et al. 2015). In addition, large earthquakes trigger many collapses and landslides, resulting in an increase in loose deposits (Lin et al. 2004; Huang and Li 2014; Yang et al. 2015; Kargel et al. 2016; Fan et al. 2018). The surface soil shrinks and cracks develop to a certain depth, resulting in high permeability and low shear strength of the soil due to intense drying and wetting cycles in the dry-hot valley (Morris et al. 1992; Tang et al. 2008). These abundant loose deposits may better accommodate and explain the development of dominate debris flow. Nonetheless, this assumption remains uncertain and further disaster case is needed to verify it.

Low-frequency, catastrophic debris flow disasters have occurred frequently in recent years (Ventisette et al. 2012; Ni et al. 2014; Deng et al. 2017). However, the discharge calculated by the hydrological manual method is usually 3-10 times lower than the actual flow discharge due to channel

blockages and dam failure processes (Cui et al. 2013). Studies have shown that landslide deposits, collapse deposits, natural boulders and artificial dams in channels can block the movement of debris flows, especially in narrow gullies and sharply curved sections (Costa and Schuster 1988). Once the blockage dam fails, a large amount of loose deposits is transformed into a debris flow, which greatly increases the discharge and eventually causes catastrophic disasters downstream (Costa and Schuster 1988; Ermini and Casagli 2003; Korup 2002; Liao et al. 2013; Cui et al. 2013). Most current research focuses on the processes of landslide deposit blockage and failure (Zhou et al. 2013; Bricker et al. 2017; Zhou et al. 2019), while, few studies have focused on boulder blockages and failures. Therefore, it is necessary to select typical cases in the drought seismic zone to study the effects of the loose deposits on the initiation and amplification of debris flows.

The Aizi Valley is located in the dry-hot valley area of the Jinsha River, which is strongly influenced by tectonic activities and dry-wet cycle weather, resulting in dense faults, intense earthquakes and an abundance of loose deposits in the basin. A large-scale debris flow occurred in the Aizi Valley on June 28, 2012, which destroyed roads and buried several houses, resulting in 40 deaths (Hu et al. 2012). The aim of this paper is to study the effects of the loose deposits on the initiation and amplification processes of debris flows, which may provide a theoretical foundation for regional prediction and warnings of debris flow hazards.

1 Study Area

The Aizi Valley is located in the northeastern part of Ningnan County, Sichuan Province, southwest China (Figure 1). The valley is 5 km from the Baihetan Hydropower Station dam site. It is a primary tributary of the Jinsha River, and the basin area is 65.55 km². The main channel is 21.96 km long and deeply cut, and the average gradient is approximately 15.5%. The elevation ranges from 604 m to 3646 m, and the maximum relative height difference is 3042 m. The terrain in the upper and middle reaches of the Aizi Valley is dominated by a V-shaped channel. The channel is

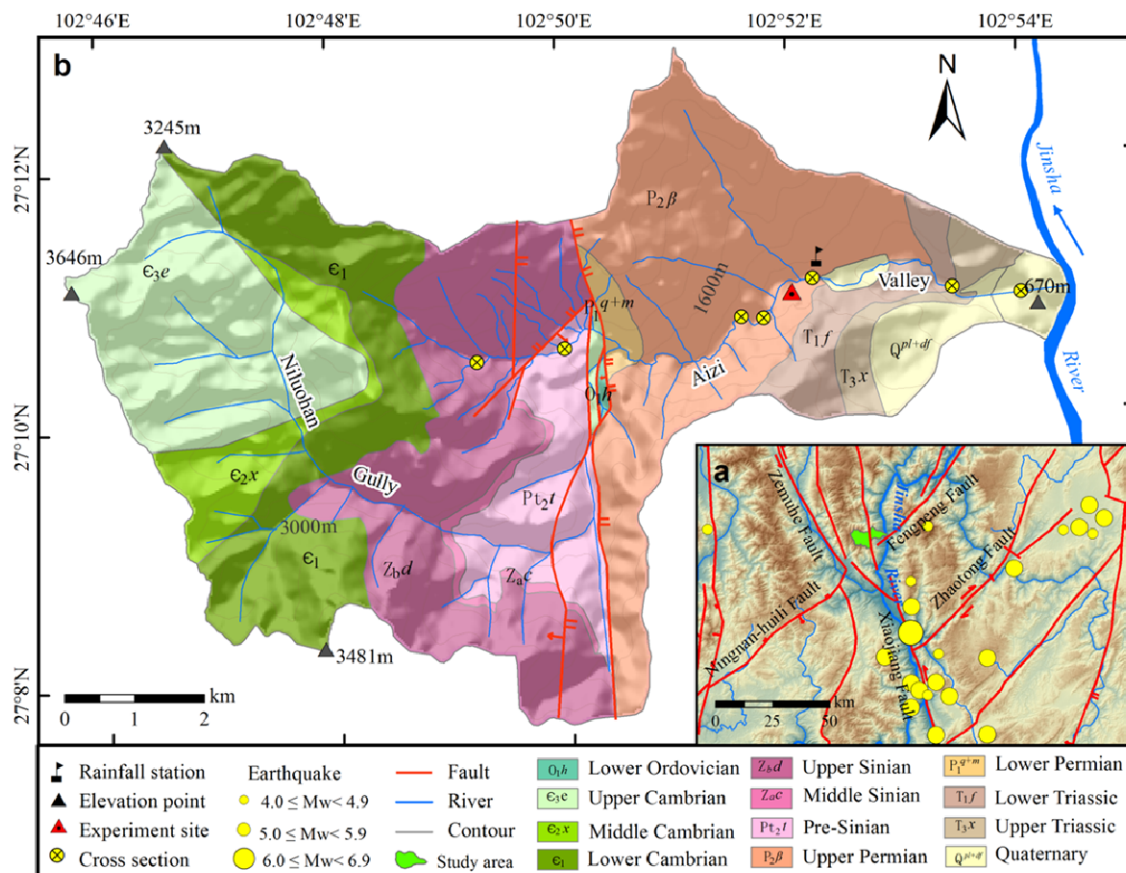


Figure 1 The location and geology map of the Aizi Valley. (a) faults and earthquakes around the Aizi Valley; (b) geology map and sites where field work was conducted.

curved and narrow, and the bank slopes are steep with a maximum slope of 66.8°. The channel gradually widens and straightens in the downstream, becoming a U-shaped valley, and the slope becomes gentle with an average gradient of 11%. Due to serious soil erosion, many cutting gullies have developed vertically on both sides of the main channel. Most of the branch gullies are small and shallow. The gully length ranges from 1~3.5 km, and the gully gradient is very steep, generally between 14.0% and 46.6%.

The Aizi Valley is located along the western part of the quasi-Yangtze plate and the northeastern edge of the Sichuan-Yunnan rhombic block, at approximately 20 km from the Xiaojiang Fault zone (Figure 1a). Folds and faults are highly developed in the Aizi Valley, and the Sikai-Jiaojihe deep reverse fault traverses the watershed. The exposed strata in the upper basin are mainly dolomite of the Upper Sinian Dengying Formation ($Z_b d$) and dolomite and sand shale of the Lower Cambrian (ϵ_1), and in the middle and lower basin,

the strata are mainly basalt of the Upper Permian Emeishan Formation ($P_2 \beta$). The basalt is overlain by sandstone and mudstone of the Lower Triassic Feixianguan Formation ($T_1 f$), and these strata are primarily exposed along both banks of the downstream section of the Aizi Valley. Sandstone and siltstone interbeds of the Upper Triassic Xujiahe Formation ($T_3 x$) and Quaternary sediments are exposed within the mouth of the Aizi Valley (Figure 1b). A debris flow stacking platform and large boulders with maximum diameters of 9.6 m scattered by debris flows in the channel were found at the outlet of the valley, which indicates that large-scale debris flows have occurred in the Aizi Valley. According to local residents, the latest debris flow occurred in 1998, and it was of medium scale. The study area is strongly affected by earthquake activity. According to statistics from the China Earthquake Network Center (<http://www.cenc.ac.cn>), there were 20 earthquakes ($M_w \geq 4.0$) in the region that affected the Aizi Valley from 1986-2011 (Figure 1b).

The basin lies in the subtropical monsoon climate zone, where the dry and wet seasons are well defined. The average annual temperature is 21.8°C, and the extreme maximum temperature is 42.0°C. The rainy season is from May to October, which accounts for more than 90% of the total annual precipitation. The temperature decreases and the precipitation increases notably as the elevation increases. Since the altitude difference of the Aizi Valley exceeds 3000 m, the change of climate with elevation is substantial. The annual rainfall amount increases with increasing elevation from 600 mm in the valley at 600 m.a.s.l. to 1600 mm in the mountain range at 3000 m.a.s.l.

2 Data and Methods

In this study, the effects of loose deposits on the formation and amplification process of Aizi Valley debris flows were revealed by analyzing the characteristics of the loose deposits and Aizi Valley debris flows. Remote sensing interpretation was used to obtain the distribution of loose deposits and vegetation coverage, and laboratory experiments were performed to analyze the particle size distribution and density of the loose deposits. Field investigations and experiments were

conducted to obtain the calculation parameters for the debris flow velocity and discharge and to explore the failure mechanics of the loose deposits on the slope. The schematic concept of the study is shown in Figure 2.

2.1 Remote sensing

Remote sensing images were used to interpret the vegetation and soil source distribution of the debris flows. To eliminate the impact of clouds, two high-resolution remote sensing images of GaoFen1 (GF1) during sunny days before and after the debris flow event were collected on May 20, 2012 and December 7, 2013, respectively. The images were obtained from the China Centre for Resources Satellite Data and Application (<http://www.cresda.com/CN/>). The resolution of the panchromatic band of the GF1 PMS is 2 m, and the resolution of the multi-spectral band is 8 m. Orthorectification, geometric correction and image sharpening were performed before interpretation under ENVI 5.2. After image sharpening, the resolution was 2 m. Manual visual interpretation was used to identify the distribution of landslides, collapses and other loose deposits. The interpretation results were checked and modified based on a field investigation.

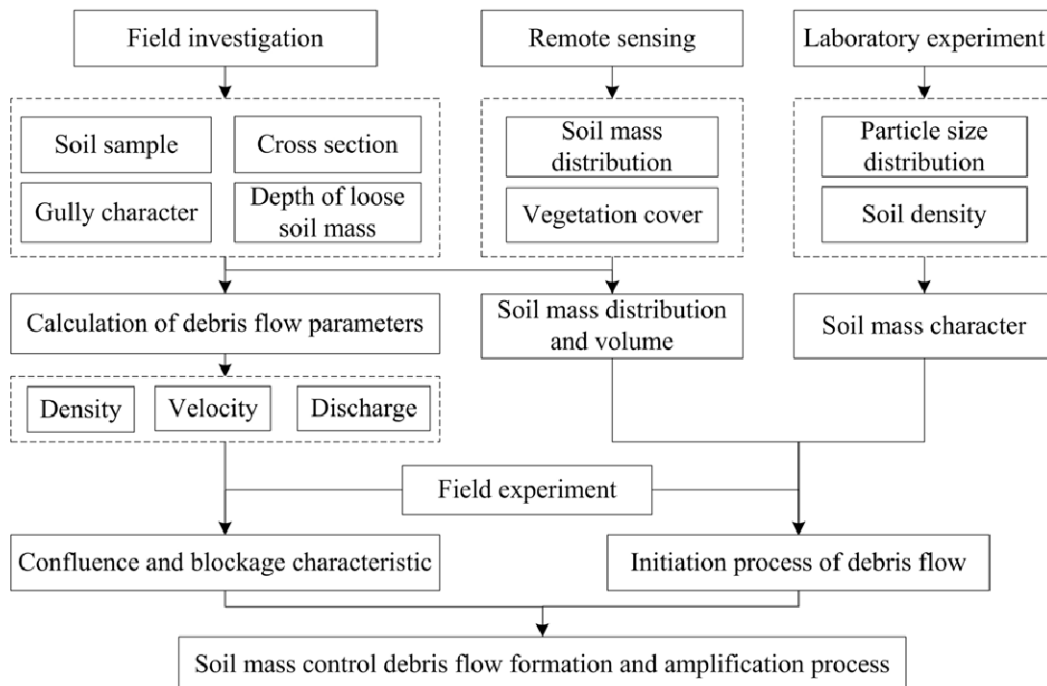


Figure 2 The schematic method concept for determining the effects of loose deposits on the debris flow process.

2.2 Field investigation

A field investigation was conducted one day after the debris flow occurrence. The field investigation included measurements of the cross section and channel gradient, collections of debris flow deposit samples and surveys of the loose deposits and blockages. To calculate the peak flow discharge, seven channel cross sections were chosen for measurements in relatively straight and smooth channels due to the nonuniform velocity of the debris flow at the bend (Figure 1c). The debris flow depth was identified based on mud marks left on the valley banks. The cross sections and channel gradient measurements were obtained using a laser range finder with an accuracy of 0.1 m. The loose deposits were checked in the field investigation, and the depth of eluvium on the slope was estimated in the outcrop.

The debris flow particle composition and bulk density can be obtained by analyzing debris flow deposits. Therefore, the dimensions and distribution of cobbles and boulders in the deposits were measured using a tape along the channel over a length of 50 meters. Grain size distribution samples were collected from debris flow deposits, as well as from the source, and measured using sieve analysis, and particles with diameters of less than 0.25 mm were measured using a Malvern laser particle size analyzer. In addition, during the field survey, some large boulders (diameter >1 m) were found in the middle reaches of the channel, which caused obvious debris flow depth variations between the upstream section and downstream sections. The numbers, dimensions and locations of these large boulders were also measured and recorded.

2.3 Field experiment

To explain the initiation mechanism of slope debris flows, an artificial rainfall-initiated debris flow experiment was conducted on a slope of the Aizi Valley in the downstream area (Figure 1c). The field experiment model was based on the slope debris flow in the Aizi Valley on June 28, 2012. Considering that the slope varied greatly in the initiation area, a rough similarity model was assumed. The hypothesis was that the slope was straight and flat, while the thickness of the loose deposits was equal, and no lateral seepage occurs. According to field investigations, the slope ranged from 20° to 55°, and the typical slope of 35° was set as the model slope angle. The slope length was 80~300 cm, and the length scale was 1:00 based on the typical slope length of 230 m. The thickness of the loose deposits was 2~5 m, and the depth scale was 1:10 based on the typical depth of 3 m.

An experiment was conducted with a slope of 35°, a length of 2.3 m, a width of 1.5 m, and an average thickness of 30 cm (Figure 3). Loose deposits were collected for the experiment from the debris flow source area to ensure that the grain composition and size distribution of loose deposits had the maximum possible similarity. Due to the model size limitations, cobbles and boulders were removed and the loose deposits were accumulated on a soil slope, with a fine particle surface on the slope top and coarse and naturally loose particles at the slope toe. The soil density was set as 1.75 g/cm³, which was the same as that of the soil source of the Aizi Valley debris flow. However, a certain error was caused by uncontrollability in the process of stacking the slope. After accumulation of the experimental section was complete, the soil

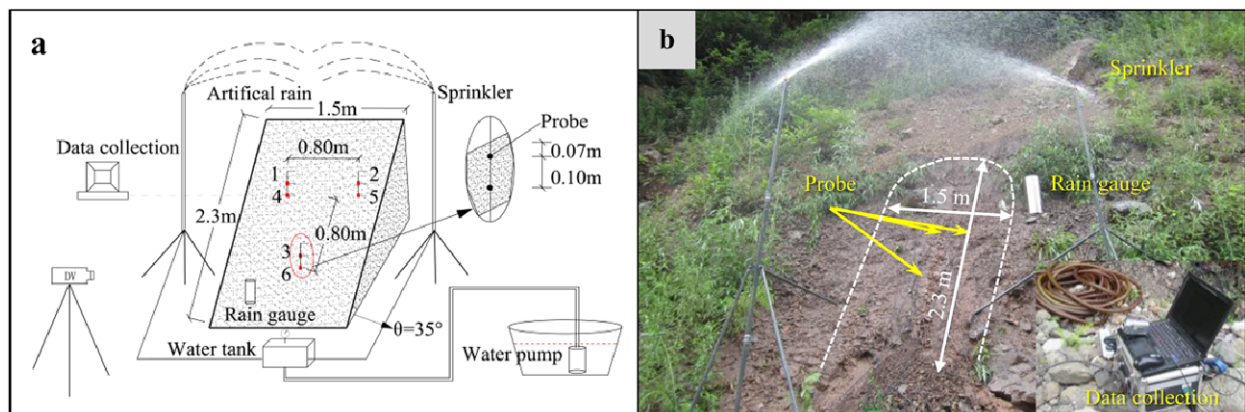


Figure 3 Debris flow triggering experiment with artificial rainfall. (a) experimental layout and (b) experimental site.

density was measured with a range of 1.75-1.82 g/cm³ and the average density was approximately 1.78 g/cm³. Three sets of water content and pore water pressure sensors were placed at distances of 0.75 m and 1.55 m from the top, respectively, and the horizontal and vertical distances between them were 80 cm. Each set included two sensors buried at depths of 7 cm and 17 cm, respectively, because slope debris flows were usually initiated by shallow failure (Gabet and Mudd 2006; Hürlimann et al. 2015), and soil permeability experiments showed that air forcing its way up through the porous media at a depth of 7 cm requires less pressure than air at a depth of 17 cm (Latifi et al. 1993). Two rain sprinklers with adjustable rain intensity were installed, and the rainfall height was 3 m from the ground. The artificial rainfall intensity was set as 77.2 mm/h according to the historical maximum rainfall recorded by the local meteorological station (Sichuan Hydrological Manual 1984). Finally, after the experiment, the average rainfall intensity measured by the rain gauges was 75.2 mm/h.

2.4 Calculation of debris flow parameters

The debris flow discharge calculation included two parts, the Aizi Valley discharge (main channel) and the gullies debris flow discharge. In the main channel, some the muddy marks were left on the bedrock banks clearly, thus indicating that the debris flow was a uniform steady flow. Therefore, the flow discharge was calculated by Eq. (1):

$$Q_c = A_c \times V_c \tag{1}$$

where Q_c is the debris flow discharge, m³/s; A_c is the section area, m², and the value was directly measured in the field investigation; and V_c is the debris flow velocity, m/s, as calculated by Eq. (2), which is commonly used in the prevention and control of viscous debris flows in mountain areas of southwest China:

$$V_c = \frac{1}{n} R_n^{2/3} I_c^{1/2} \tag{2}$$

where n is Manning’s roughness coefficient; R_n is the hydraulic radius, m; and I_c is the channel gradient. The Manning’s roughness coefficient in this paper is approximately evaluated based on the research work of Xu and Feng (1979). Considering a viscous debris flow, and its comparatively straight

channel, therefore, the roughness coefficient of Aizi Valley debris flows can be approximately evaluated as 0.08. The values of R_n , and I_c were measured in the field investigation.

In the gully debris flows, the bed and banks were severely eroded, and obtaining accurate sections of muddy marks was impossible. Therefore, the discharge of the gully debris flow was calculated by the empirical equation recommended by the Specification of Geological Investigation for Debris Flow Stabilization in China (T/CAGHP 006-2018). The method was based on the assumption that solid material joins the water flood and amplifies the flood magnitude as shown in Eq. (3):

$$Q_c = (1 + \phi) Q_w D_u \tag{3}$$

where D_u is the blockage coefficient in the debris flow gully, and its value is based on the channel characteristic obtained from the field investigation compared to the recommended value in a lookup table (Wu et al. 1993). The degree of blockage is classified into four categories in the lookup table, i.e., very serious blockage ($D_u=3.0\sim2.5$), serious blockage ($D_u=2.5\sim2.0$), normal blockage ($D_u=2.0\sim1.5$), and minor blockage ($D_u=1.5\sim1.0$). In this study, the slope gully blockage was considered to be a normal blockage ($D_u=2.0\sim1.5$) and the value was set at a medium value of 1.8.

Q_w is the flood peak discharge and can be calculated from Eq. (4), which is based on the rainfall force S (mm/h) (Rainstorm runoff calculation method in small watershed, 2010). This method is widely used in southwest China because of the easy access to related parameters in the lookup table, although the method depends on the specific conditions of each catchment area (Zhou et al. 1991; Liu et al. 2013, 2014; Guo et al. 2019).

$$Q_w = 0.278 \psi \frac{S}{\tau^n} F \tag{4}$$

where, F is the watershed area of the debris flow gully, km²; ψ is the runoff coefficient of the flood peak discharge; s is the rainfall intensity, mm/h; τ is the runoff confluence time of rainstorm h; and n is the attenuation index of the rainstorm. The parameters and calculation process are explained in detail in the appendix 1.

ϕ is the amplification coefficient of the debris flow peak discharge, which can be calculated from

Eq. (5).

$$\phi = (\gamma_c - \gamma_w) / (\gamma_s - \gamma_c) \quad (5)$$

where, γ_s is the specific gravity of the soil, g/cm³ and the value is set as 2.65 g/cm³ due to the distribution of the nine gullies in the Upper Sinian dolomite area (Figure 1), where the density of dolomite is 2.4-2.9 g/cm³; thus, an average density is set. γ_w is the unit weight of water, $\gamma_w = 1$ g/cm³, and γ_c is the unit weight of the debris flow, g/cm³, which can be calculated from Eq. (6).

The flow rate of debris flow is difficult to determine after the occurrence of a disaster. The information stored in debris flow deposits is generally used to estimate the debris flow density. In this paper, Chen’s method (Chen et al. 2003) was used to estimate the debris flow density, which is widely used in debris flow studies in southwest mountainous areas (Hu et al. 2016; Zou et al. 2017). This method is established based on the

relationship between the clay content (<0.005 mm) and the debris flow density of 45 debris flow gullies in southwestern China because 13 debris flow gullies are located very close to the Aizi Valley.

$$\gamma_c = -1.32 \times 10^3 x^7 - 5.13 \times 10^2 x^6 + 8.91 \times 10^2 x^5 - 55x^4 + 31.6x^3 - 67x^2 + 125x + 1.55 \quad (6)$$

where, x is the clay particle content of the debris flow, and its value is based on measurements of debris flow soil samples using a Malvern laser particle size analyzer.

3 Results

3.1 Loose deposits preparation phase

A large number of loose deposits were distributed in the Aizi Valley. According to remote sensing and field survey data, the loose deposits include (i) eluvium on the slope, (ii) landslide

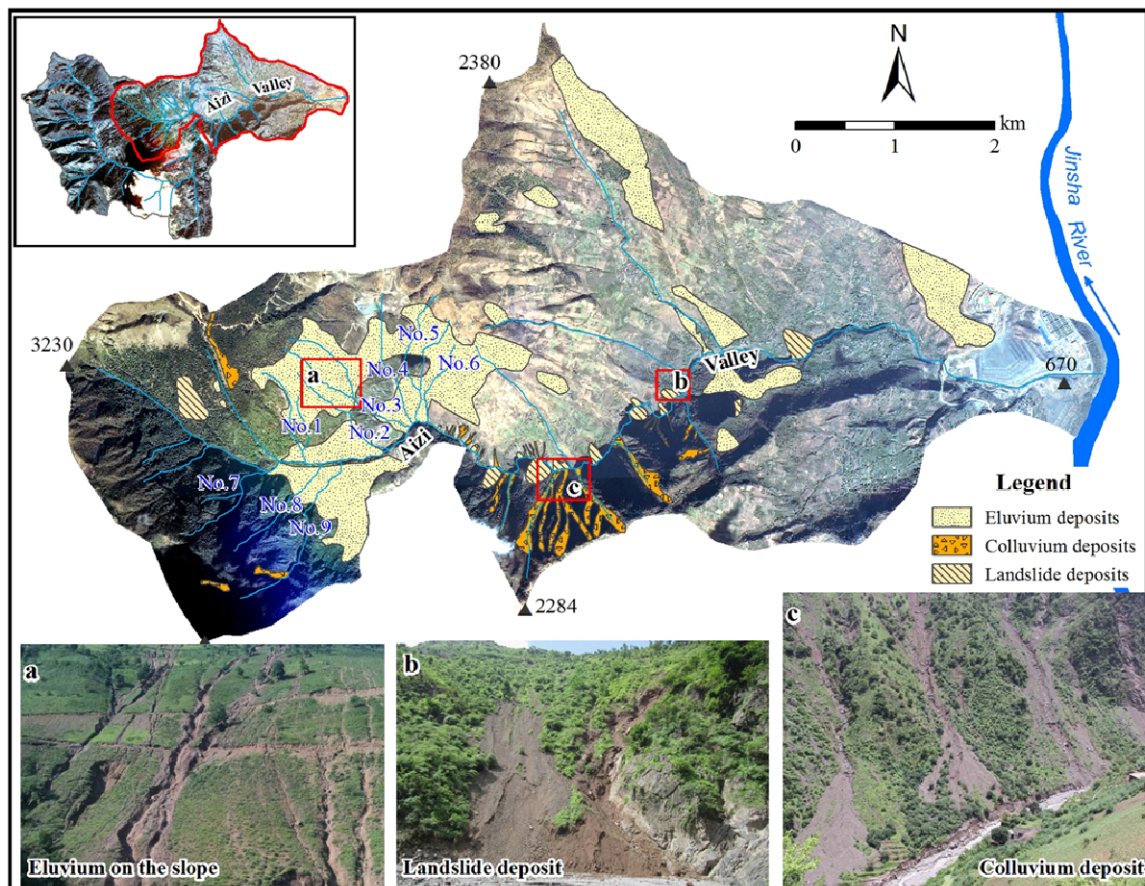


Figure 4 The loose deposits distribution in the Aizi Valley. (a) Eluvium on the slope and developed gullies; (b) landslide deposit along the main channel; and (c) colluvium deposit along the main channel.

deposits and (iii) colluvium deposits, with a total area of 5.01 km² and a volume of approximately 23.54×10⁶ m³ (Figure 4).

Eluvium is mainly distributed on the left bank of the valley, particularly near the fault zone. These deposits accumulate on the gentle slope and low-lying terrain and show a decreasing trend from the bottom to the top of the slope. The thickness varies from 2 m to 10 m, with a total volume of 17.38 ×10⁶ m³. Due to poor vegetation cover and strong dry and wet cycles, the surface is subjected to strong erosion, which results in the formation of gullies (Figure 4a). The slope eluvium is the most important source of debris flow formation.

Landslide deposits are mainly distributed on the banks of the gullies (Figure 4b). Thirteen landslides are distributed along the channel, and these landslides are generally small. The total volume is 4.08 ×10⁶ m³, which is estimated using a power-law landslide area-volume empirical formula (Larsen et al. 2010). Although a certain error occurs in the landslide volume estimated by the empirical formula, the error range is within 10%. Most of the landslides are small, with volumes ranging from 4.36×10³ m³ to 1.54×10⁶ m³. The landslide deposits lying along the channel are prone to adding to debris flow movement.

Colluvium deposits are mainly distributed on both sides of the middle reach of the valley (Figure 4c). These deposits have average thicknesses of 2 m in the upper part and 7 m at the bottom of the slope, with a total volume of approximately 2.07×10⁶ m³. The colluvium deposits lying at the slope bottom can easily contribute to debris flow movements.

Not all loose deposits can participate in the debris flow movement process. Studies have shown that only low-density loose deposits with a wide grain size distribution and medium clay content are favorable for debris flow initiation (Chen et al. 2010; Iverson et al. 2005). Laboratory experiments show that the average loose deposits density in the debris flow source area is 1.75 g/cm³, which is a low density. The particle size distribution indicates that the loose deposits have a medium clay content of 2.1% ~ 3.8% (Figure 5). According to the field investigation, large amounts of slope

eluvium contributed to the slope debris flow initiation and gully debris flow, while only a small part of landslide deposits and colluvium deposits at the bottom of slope were eroded and entrained into the debris flow in the main channel.

Antecedent droughts and earthquakes affected the particular characteristics of the soil mass and may have increased the potential debris flow loose deposits in the Aizi Valley. The standard precipitation index (SPI) proposed by McKee et al. (1993) was used to assess the degree of drought in the Aizi Valley. The interseasonal scale SPI was calculated based on the monthly rainfall data of Ningnan County, and the drought degrees were classified into five categories (Fiorillo et al. 2012): near normal (-0.5 < SPI ≤ 0.5), mild drought (-1.0 < SPI ≤ -0.5), moderate drought (-1.5 < SPI ≤ -1.0), severe drought (-2.0 < SPI ≤ -1.5), and extreme drought (SPI ≤ -2.0). The results indicate that the Aizi Valley has a strong dry-wet cycle (Figure 6). The Aizi Valley suffered drought nearly every year, with 2000, 2002, 2004, 2005 and 2007 recording severe droughts and 2010 to 2012 recording extreme droughts. The severe droughts reduced the vegetation cover, weakened the soil strength and increased soil cracks, which resulted in particularly strong soil erosion during dry years (Wei et al. 2011; Han et al. 2018). These droughts can explain why strongly eroded slopes and gullies were found in the Aizi Valley (Figure 4a). In addition, the long-term dry-wet cycle accelerates rock weathering,

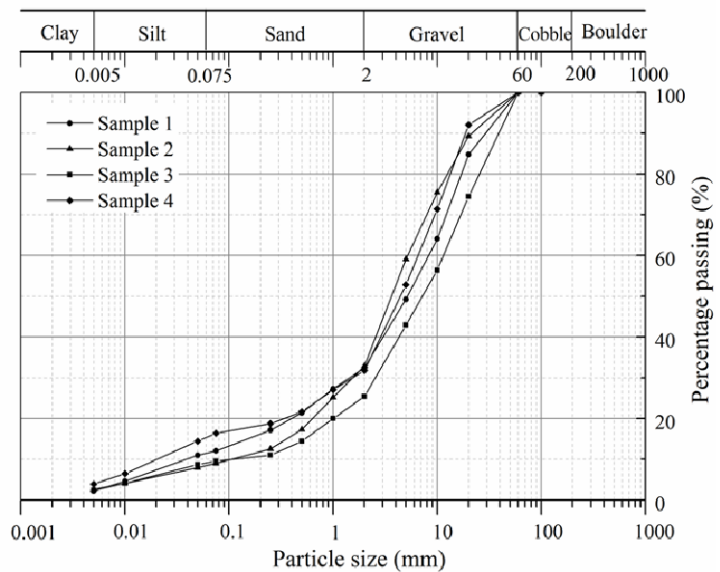


Figure 5 Particle size distribution of the loose deposits in the debris flow source area.

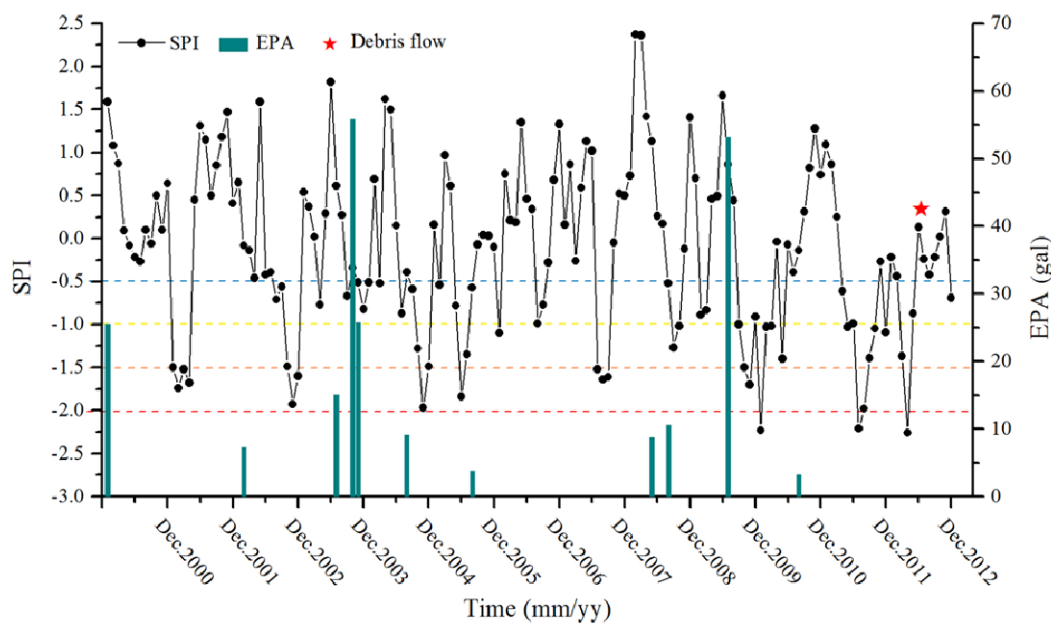


Figure 6 The standard precipitation index (SPI) and effective peak acceleration (EPA) results from 2000 to 2012. The different colored dotted lines represent dryness threshold values, blue (mild drought), yellow (moderate drought), orange (severe drought) and red (extreme drought).

causing the rock to break down into loose debris, forming soil with a wide grain size distribution (Chen et al. 2014). The Aizi Valley is located in the Anninghe seismic belt, where frequent earthquakes increase the amount of potential loose deposits. Thirteen earthquakes ($M_w \geq 4.9$) occurred near the Aizi Valley between 2000 and 2011 according to the database of the National Earthquake Data Center. The effective peak acceleration (EPA) of earthquake was used to assess the effects of the seismic events (Yu and Gao 2001). The results show that the earthquakes in Oct. 2003 and Jul. 2009 strongly affected the Aizi Valley, and both values were over 50 gal (Figure 6). Previous studies showed that earthquakes produced many loose deposits with high infiltration rates and unconsolidated characteristics, which result in an increasing frequency and size of debris flows, such as those associated with the Chi-Chi earthquake (Lin et al. 2004) and the Wenchuan earthquake (Huang et al. 2014; Fan et al. 2019). In addition, earthquakes make loose deposits looser, which increases the effective debris flow source (Chen et al. 2014). The combined effects of the earthquakes in 2009 and 2010 and the extreme droughts in 2010-2012 increased the potential loose deposits amount for debris flow preparation.

3.2 Slope debris flow initiation phase

Loose soil failures lead to slope debris flow formation in the Aizi Valley. Although there was routine seasonal rainfall during the debris flow formation, this routine rainfall was not the controlling factor in the Aizi Valley. The rainfall data were collected from the nearest meteorological station, the Xintian station ($102^{\circ}53'10.81''E$, $27^{\circ}13'32.29''N$, 1240 m), and showed that from 20:00 on June 27 to 8:00 on the 28th, the rainfall amount reached a total of 76.9 mm. The average rain intensity during this period was 13.2 mm, and the maximum hourly rainfall intensity was 23.3 mm occurred between 5:00 and 6:00 (Figure 7). This rainfall represents a 10-year recurrence period according to the rainfall probability distribution (Zhang 2004). After the debris flow occurred, a rain gauge station was built in the downstream reach of the Aizi Valley (Figure 1). The monitoring data from 2013 to 2015 show that there were two heavy rainfall processes that triggered flash floods on July 18, 2013 and July 15, 2015, with maximum hourly rainfall intensities of 22.5 and 48.6 mm, respectively (Figure 7). The hourly precipitation amounts that triggered the Aizi Valley debris flows are of high frequency in this region. Therefore, this rainfall can easily meet the formation conditions of a debris flow.

The experiment on artificial rainfall triggering debris flows shows that the water content and pore

water pressure are the key factors controlling debris flow initiation. Based on the various water contents and pore water pressures (Figure 8a), the soil on the slopes of the Aizi Valley experienced five stages during transformation into a debris flow under rainfall conditions, including heavy rainfall infiltration, runoff yields in excess of infiltration, soil saturation, the initiation of soil creep and slope debris flows.

(i) Heavy rainfall infiltration: At the beginning of the rainfall, a large amount of rainwater infiltrated into the soil, and some fine fissures appeared at the top of the soil surface. The soil at

the toe of the slope was squeezed; however, no surface runoff was formed. At this stage, the water content and pore water pressure both showed minor changes, with the water content increasing from 9.1% to 11.5% and the pore water pressure increasing from 0 to 0.006 kPa. The slope remained stable at this stage.

(ii) Runoff yield in excess of infiltration: As the precipitation continued, the soil water content increased, the infiltration rate gradually decreased, and the final rainfall rate exceeded the infiltration rate to produce runoff. The water content increased from 11.5% to 18.1%, and the pore water pressure

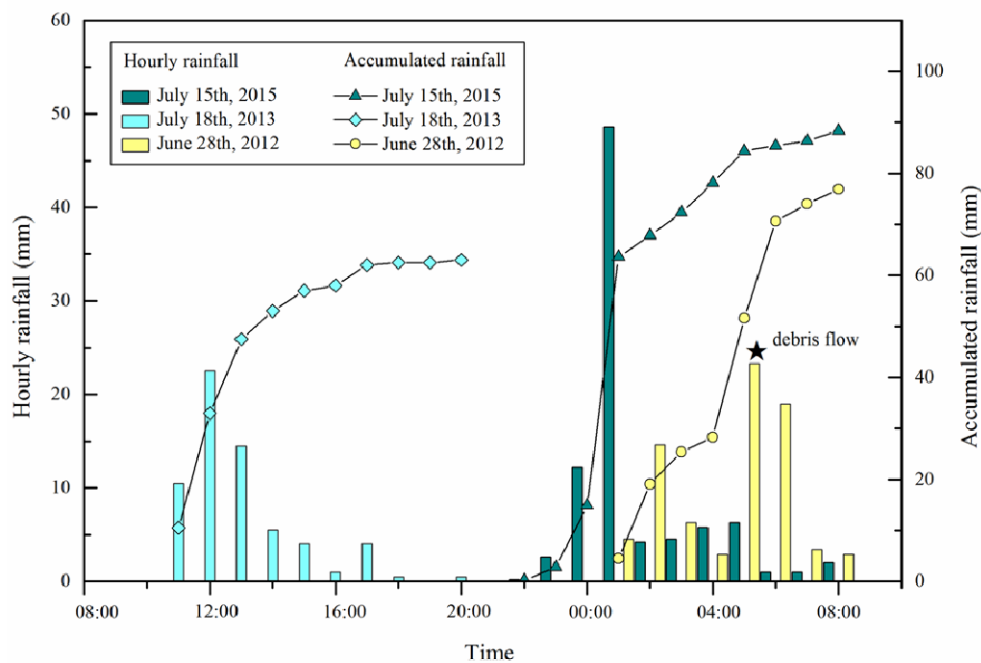


Figure 7 Rainfall before the Aizi Valley debris flow event recorded by the Xintian rain gauge station and rainfall before the 2013 and 2015 flash flood events recorded by the Aizi rain gauge station.

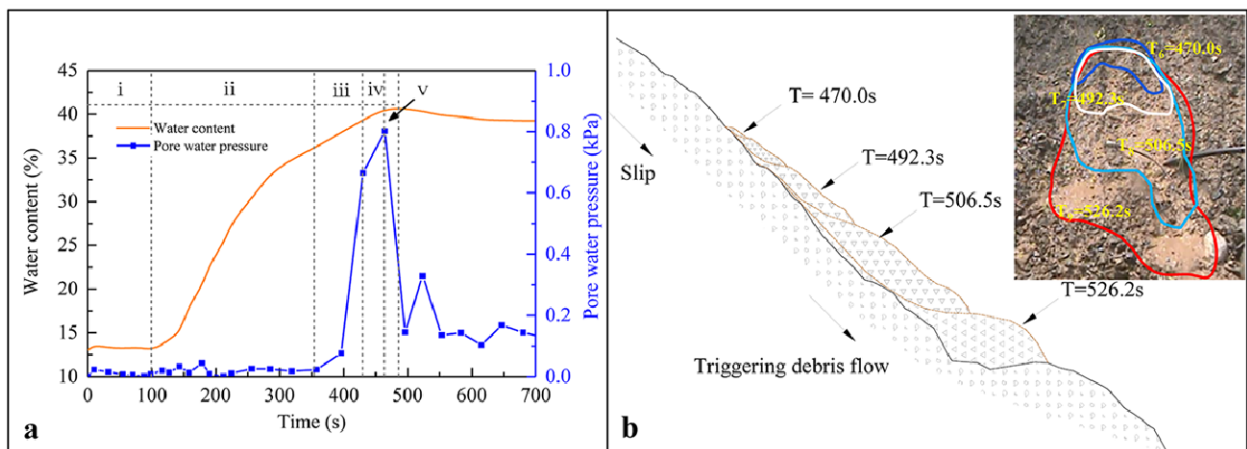


Figure 8 (a) Time series of water content and pore water pressure, indicating 5 stages of a slope debris flow. (b) Sketch map of slope failure at different times.

increased from 0.006 kPa to 0.013 kPa. The runoff yield in excess of infiltration promoted the increase of the topsoil water content, while the yield decreased the cohesion force and thus reduced the soil stability.

(iii) Soil saturation: With an increase in the water content to 23.4% and a pore water pressure increase to 0.678 kPa, the soil gradually became saturated, which decreased the cohesion and angle of internal friction of the soil and thus resulted in further reduction of the shear strength and soil stability.

(iv) Soil creep formation: At this stage, the pore water pressure of the soil increased to 0.727 kPa, and cracks developed at the back scarp of the slope, which provided favorable conditions for soil creep formation.

(v) Initiation of slope debris flow: The pore water pressure of the soil continued to rise and reached 0.752 kPa at this stage. The decrease of the soil cohesion resulted in the reduction of the soil shear strength, which caused the soil to slide. The soil moved down and transformed into a slope debris flow. Notably, the particles showed a significant relationship with the soil movement. The experiment on slope debris flow generation

from soil creep lasted for 56.2 seconds, and the failure process is shown in Figure 8b.

3.3 Debris flow confluence and discharge amplification phase

According to the field investigation, there are nine debris flow gullies distributed between cross section 1 and cross section 3 (Figure 4). The confluence of these debris flows occurs in the Aizi Valley to complete the valley debris flow formation (Figure 9). These gully basins are small, with areas of 0.21 km² ~ 6.5 km², the average channel gradient is 45.9%, and the middle and lower reaches of the basins are developed mostly on the eluvium slope. Therefore, debris flows eroded the gully bed and banks along the steep slope, making the gully deeper and wider (Figure 9a). The peak discharge at each gully is calculated by the hydrological manual method, and the results are shown in Table 1. Gully no. 9 is the largest, with a peak discharge of 39.03 m³/s, while gully no. 2 is the smallest, with a peak discharge of only 6.15 m³/s. After the confluence of all nine gullies and under the action of erosional processes, the Aizi Valley fresh water discharge increased from 38.67 m³/s to the debris

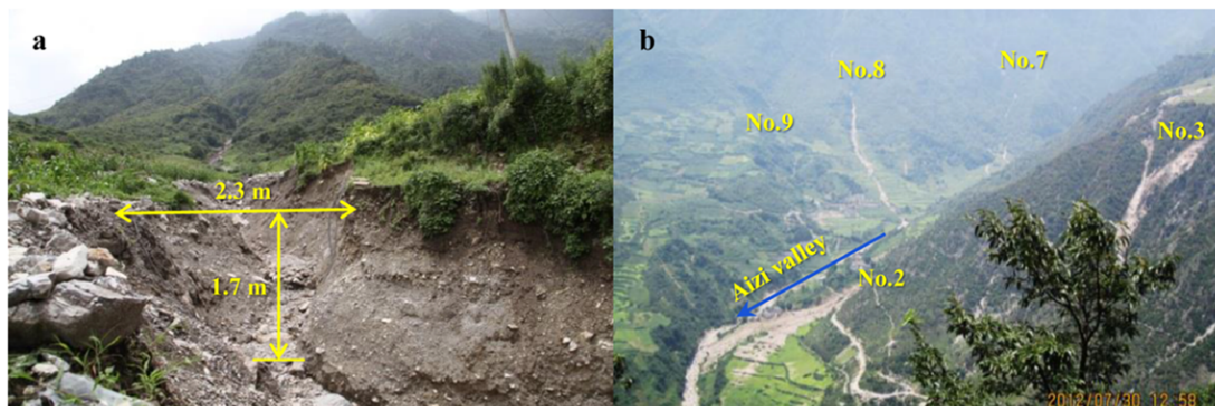


Figure 9 Photographs of gully debris flow confluence into the Aizi Valley; (a) No. 1 gully debris flow developed on the eluvium slope and (b) confluence of all nine gullies into the Aizi Valley.

Table 1 Characteristic parameters and discharge of nine debris flow gullies

Number	Location		Area (km ²)	Length (km)	Gradient (%)	Discharge (m ³ /s)
No. 1	27°10'31"N	102°49'30"E	0.43	1.3	49.8	18.18
No. 2	27°10'34"N	102°50'00"E	0.22	1.68	45.5	6.15
No. 3	27°10'41"N	102°50'7"E	0.66	1.78	43.8	22.92
No. 4	27°10'43"N	102°50'9"E	0.68	1.61	40.4	25.1
No.5	27°10'45"N	102°50'11"E	0.69	1.45	34.9	27.04
No.6	27°10'43"N	102°50'15"E	0.21	1.09	41.9	8.23
No.7	27°10'29"N	102°49'19"E	0.41	1.26	62.7	18.9
No.8	27°10'26"N	102°49'33"E	0.43	1.19	56.3	19.94
No.9	27°10'24"N	102°49'40"E	1.31	2.49	38.1	39.03

flow discharge of 255.2 m³/s (Figure 10).

The debris flow parameter calculations taken from seven sections of the valley are shown in Table 2. The discharge increased sharply from 255.27 m³/s to 835.56 m³/s, the cross section area increased by 1.95 times and the velocity increased by 1.68 times within a short distance of 0.45 km. A flow discharge surge within such a short distance is usually caused by blockage amplification (Cui et al. 2013; Zhou et al. 2013). The field investigation shows that there was no gully confluence or large landslide between sections 3 and 4. However, a large basalt boulder of 7.2 m×6.1 m×8.5 m was found (Figure 11b, c), which gives a clear indication of the discharge increase due to boulder blockage and outburst. A large boulder partially blocked the valley, making the valley narrower, and only 2 m of

space was left for the passage of the debris flow; however, boulders carried by the debris flow from upstream could not pass through this narrow section with a very gentle slope of 13°, which resulted in complete blockage of the valley. The Aizi Valley has a viscous debris flow with a bulk density of 1.8 g/cm³, which cannot easily pass through the minute gaps in the temporary dam (Yu et al. 2013). A continuous debris flow influx increased the pressure on the temporary dam walls, which ultimately burst and led to a debris flow discharge surge.

The basalt of the Emeishan Formation (P₂β) in the middle reaches of the Aizi Valley provided a favorable environment for valley blockage. These basalts have columnar fractures cross-cut by three sets of joints (Figure 11a), which can easily be

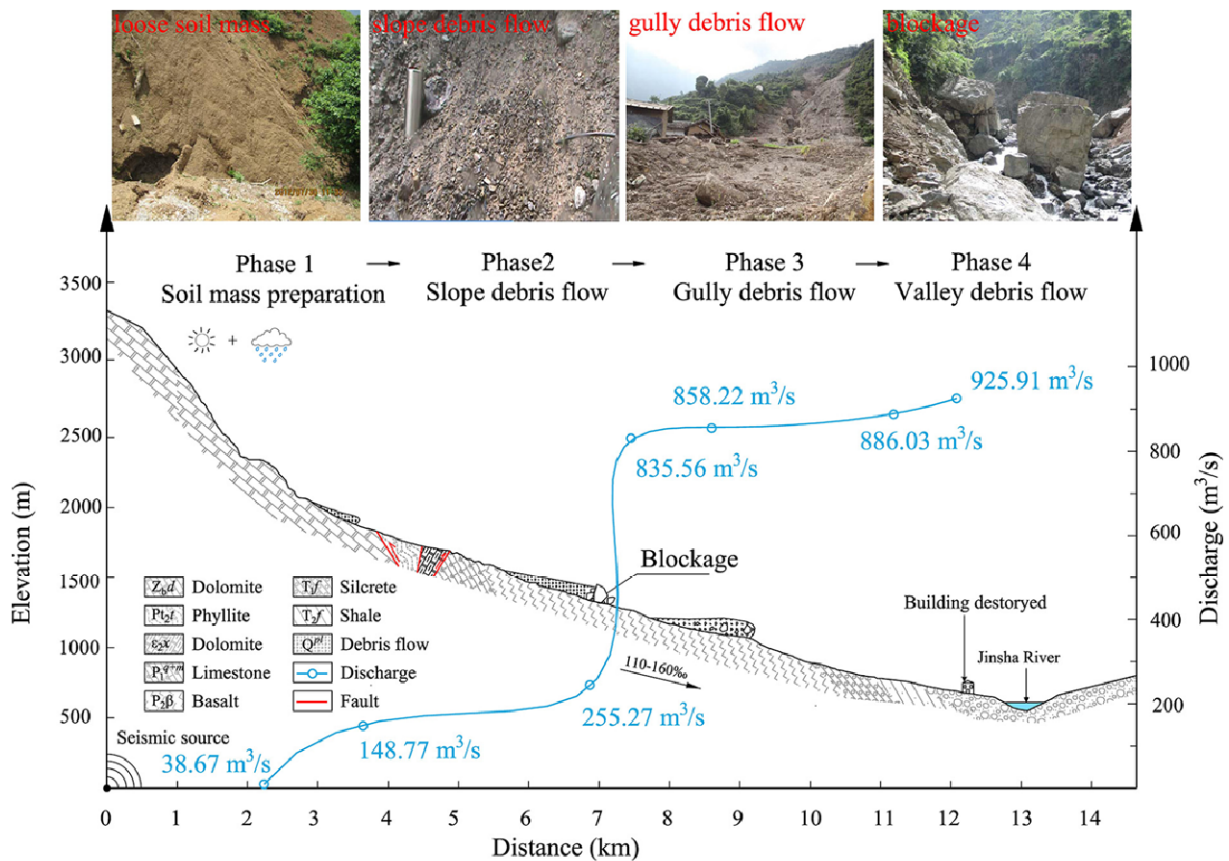


Figure 10 The initiation and amplification processes of Aizi Valley debris flow.

Table 2 Calculation of debris flow discharge in seven cross sections

Cross section	1	2	3	4	5	6	7
Area (m ²)	7.61	23.25	34.50	67.38	81.74	82.81	80.23
Mud depth (m)	1.13	1.06	1.98	4.76	3.71	4.29	4.28
Slope (°)	8	8	8	7	7	6	7
Velocity (m/s)	5.08	6.4	7.4	12.4	10.5	10.7	11.54
Discharge (m ³ /s)	38.67	148.77	255.27	835.56	858.22	886.03	925.91



Figure 11 The boulder development environment and blockage site. (a) Columnar joint of the Emeishan basalt around the blockage site. (b) The blockage site in the middle reach of Aizi Valley. (c) The large basalt boulder left in the valley. (d) Large boulders moved by the debris flow.

broken from the source rock and participate in the Aizi Valley debris flow, ultimately blocking the narrow section of the valley. This mechanism was confirmed through field investigations, in which many boulders were found scattered along the valley, and 60% of the deposits in the debris flow deposition zone were basalt. Two large basalt boulders were found to have sizes of $7.1\text{ m}\times 4.3\text{ m}\times 3.9\text{ m}$ and $5.5\text{ m}\times 4.2\text{ m}\times 3.5\text{ m}$ in the deposition zone (Figure 11d). Therefore, the large boulders that developed in the basalt dominated the discharge amplification process of the Aizi Valley debris flow.

4 Discussion

According to our study, loose deposits is well documented as the most important factor affecting all of the debris flow processes of the Aizi Valley, especially for the discharge amplification process. Here, the phenomenon of discharge amplification caused by boulder blockage and failure is discussed.

Traditionally, it is believed that soft rock areas are prone to forming debris flow hazards (Wei et al. 2008). However, studies have found that low-

frequency debris flows mainly occur in hard rock areas, which often lead to destructive damage (Lu et al. 2011; Yu et al. 2014). For example, a catastrophic debris flow occurred in the Sanyanyu Gully of Zhouqu, China (August 8, 2010), which is a limestone bedrock zone (Cui et al. 2013). The Venerilla debris flow (December 1999) in 1999, which caused approximately 30,000 deaths, occurred in the strong granite bedrock zone (Francisco 2001). Studies have indicated that the most devastating debris flows are related to amplification from channel blockages and failures (Costa and Schuster 1988, Korup 2005). The fatal debris flow in the Aizi Valley is a good example of discharge amplification caused by boulder blockage and failure, while it is totally different from the landslide deposits caused by blockage and amplification.

Landslides occur more often in soft rock areas, and when a landslide reaches the bottom of a river, the unconsolidated heterogeneous mixture of earth and rock debris forms a dam that completely or partially blocks the channel (Costa and Schuster 1988). However, boulder blockages are more prone to occur in hard rock areas. Because hard rock

areas are more prone to collapses and rockfall, it is difficult for floods to move large boulders downstream, which leads to boulders accumulating and crowding some parts of the channel without completely blocking the water flow. During the movement of a viscous debris flow, coarse particles are mainly concentrated in the head, and these large particles would be stopped when the channel becomes narrow or the gradient decreases (Inverson et al. 1997; Cui et al. 2015). In addition, the yield stress of a viscous debris flow is large (Jeong 2014); thus so the shear force cannot easily reach the critical viscous resistance, which causes the fluid to not be able to easily flow through the gap. Therefore, the coarse particles of the viscous debris flow and large boulders constitute a temporary blockage dam.

According to Costa and Schuster (1988) and Cui et al. (2013), the variation of discharge amplification caused by natural dam failure is positively related to the potential energy of flow water/debris flow behind the dam, and the potential energy of water/debris flow behind the dam can be calculated as the product of dam height, volume, and the specific weight of water/debris flow. This theory can also be used to explain the discharge amplification resulting in boulder blockage dam failure. Thus, the differences in the amplification of peak discharges caused by natural dam failures appear to be controlled by the dam characteristics (i.e., the type, size, geometry and material composition) (Costa and Schuster 1988). For a boulder blockage dam, the dam height is determined by the boulder height and the volume is mainly related to the size of the boulder. In general, the diameters of boulders range from a few meters to dozens of meters. The height of the blockage boulder is 8.5 m in this study, and the maximum blockage boulder in the Taining debris flow is 12.9 m (Zhang et al. 2019). Although few studies have focused on boulder blockages, the dimension of the largest boulder carried by a debris flow can be used as a reference. Even in the large-scale ($7.5 \times 10^7 \text{ m}^3$) debris flow of Zhouqu, the diameter of the largest boulder diameter left in the depositional zone was 6.5 m (Tang et al. 2011). Additionally, the largest boulder found in another catastrophic debris flow of the Qipan gully was $15 \text{ m} \times 6 \text{ m} \times 8 \text{ m}$ (Zou et al. 2016). However, among samples of 84 landslide deposit dams (Ermini and

Casagli 2003), 67% of dams were found to be higher than 20 m, and 31% were higher than 50 m, which indicates that the scale of a boulder blockage is usually smaller than that of a landslide deposits dam. In addition, the discharge amplification of a landslide deposits dam includes not only the accumulation of flow but also landslide deposits entrainment, while a boulder blockage involves only flow accumulation. In the Aizi Valley, the peak discharge was amplified by 3.3 times due to boulder blockage and failure and can be 2~50 times greater if caused by a landslide dam blockage (Cui et al. 2013). This can also explain why scholars are more concerned about landslide deposit blockages.

In fact, the phenomenon of boulder blockages and outbursts is ubiquitous. A similar blockage phenomenon was also observed by chance during the artificial rainfall experiment. The continuous artificial rainfall first led to rill gully formation, and gravel (with a particle size of $12.5 \text{ cm} \times 7.6 \text{ cm} \times 3.1 \text{ cm}$) fell from the steep slope and blocked the narrow section of the rill gully, making a temporary dam (Figure 12a). With debris flow accumulation, the temporary dam washed away after just six seconds (Figure 12b, c). The velocity and discharge suddenly increased. The velocity increased from 31 cm/s at cross section 1 to 47 cm/s at cross section 2, and the width of the rill gully at cross section 2 increased to approximately 8.2 cm. Although this shallow and steep rill gully was not conducive to flow accumulation, which resulted in a short blockage, the amplification effect was evident.

Although the phenomenon of discharge amplification in a debris flow discharge resulting from natural dam blockage and failure has been well demonstrated in both experimental and actual debris flow cases (Theule et al. 2012; Cui et al. 2013; Zhou et al. 2013), the basic principle is quite complicated and certainly not yet fully understood.

5 Conclusion

A rainfall-triggered debris flow with a 10-year recurrence period occurred in the Aizi Valley on July 28, 2012. The loose deposits were found to dominate the initiation and amplification processes of the Aizi Valley debris flow. The loose deposits dominated the three phases of the Aizi Valley

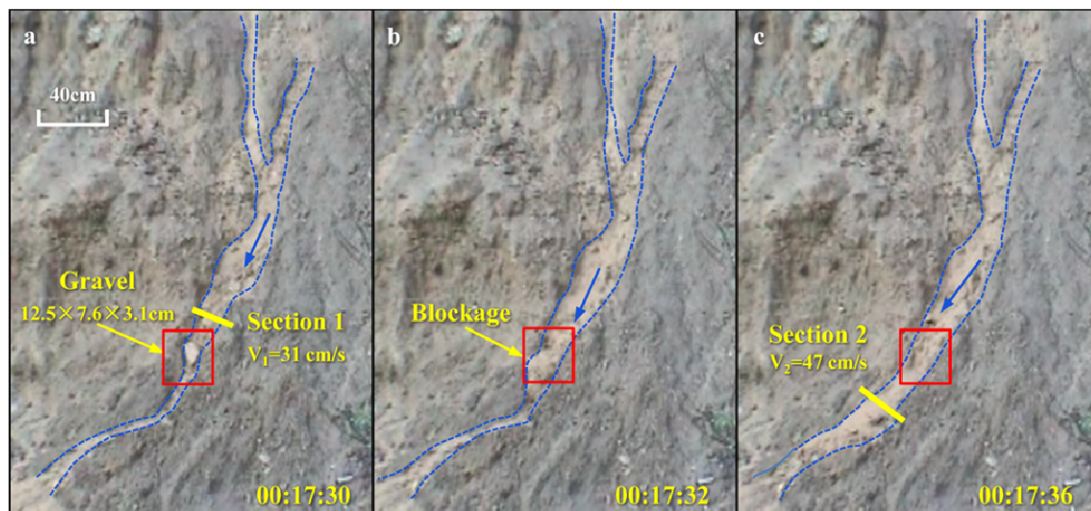


Figure 12 The gravel blockage and dam failure phenomena in the gully debris flow during the artificial rainfall experiments.

debris flow, as follows. 1) Loose deposits preparation: antecedent droughts and earthquake activities affected the soil structure and increased the potential loose soil sources in the Aizi Valley, which laid the foundation for debris flow formation; 2) Slope debris flow initiation: Rainfall and flow concentration caused the pore water pressure to increase, which led to the eluvium with a low density, medium clay content and wide grain size failing and transforming into a slope debris flow; 3) Gully debris flow confluence and valley debris flow amplification: nine gully debris flows converged into the Aizi valley, and a blockage and failure caused by a large boulder 7.2 m×6.1 m× 8.5 m in size resulted in the amplification of the debris flow discharge by 3.3 times. According to this research, the prediction of regional debris flows should consider the loose deposits to a greater degree,

especially in dry-hot valleys and seismic belts. Moreover, boulder blockages can help in predicting and assessing regional debris flows in dry-hot valleys and seismic belts. Additionally, preventative and mitigation engineering works for debris flows in hard rock areas should not ignore the effects of boulder blockages and failure.

Acknowledgements

This research was supported by the National Natural Science Foundation of China (Grant Nos. 41861134008 and 41601476), the National Key Research and Development Program of China (Grant No. 2018YFC1505202) and the 135 Strategic Program of the IMHE, CAS (Grant No. SDS-135-1705).

References

- Bricker JD, Schwanghart W, Adhikari BR, et al. (2017) Performance of models for flash flood warning and hazard assessment: the 2015 Kali Gandaki landslide dam breach in Nepal. *Mountain Research & Development* 37 (1): 5-15. <https://doi.org/10.1659/MRD-JOURNAL-D-16-00043.1>
- Chen NS, Cui P, Liu ZG, et al. (2003) Calculation of the debris flow concentration based on clay content. *Science in China Ser. E Technological Sciences* 46: 163-174. <https://doi.org/10.1360/03EZ0005>
- Chen NS, Lu Y, Zhou HB, et al. (2014) Combined impacts of antecedent earthquakes and droughts on disastrous debris flows. *Journal of Mountain Science* 11(6): 1507-1520. <https://doi.org/10.1007/s11629-014-3080-7>
- Chen NS, Yang CL, Zhou W, et al. (2011) Investigation technology for debris flow. Beijing, science press. pp 76-80.
- Chen NS, Zhou W, Yang CL, et al. (2010) The processes and mechanism of failure and debris flow initiation for gravel soil with different clay content. *Geomorphology* 121(3-4): 222-230. <https://doi.org/10.1016/j.geomorph.2018.01.012>
- Costa JE, Schuster RL (1988) Formation and failure of natural dams. *Bull Geol Soc Am. Geological Society of America Bulletin* 100(7): 1054-1068. [https://doi.org/10.1130/0016-7606\(1988\)100<2.3.CO>2](https://doi.org/10.1130/0016-7606(1988)100<2.3.CO>2)
- Cui P, Zeng C, Lei Y (2015) Experimental analysis on the impact force of viscous debris flow. *Earth Surface Processes and Landforms* 40(12): 1644-1655. <http://doi.org/10.1002/esp.3744>
- Cui P, Zhou GGD, Zhu XH, et al. (2013) Scale amplification of natural debris flows caused by cascading landslide dam failures. *Geomorphology* 182: 173-189.

- <https://doi.org/10.1016/j.geomorph.2012.11.009>.
Deng MF, Chen NS, Liu M. (2017) Meteorological factors driving glacial till variation and the associated periglacial debris flows in Tianmo Valley, south-eastern Tibetan Plateau. *Natural Hazards and Earth System Science* 17(3): 345-356. <https://doi.org/10.5194/nhess-17-345-2017>
- Ermini L, Casagli N. (2003) Prediction of the behavior of landslide dams using a geomorphological dimensionless index. *Earth Surface Processes and Landforms* 28 (1): 31-47. <http://dx.doi.org/10.1002/esp.424>
- Fan X, Scaringi G, Qiang X, et al. (2018) Coseismic landslides triggered by the 8th August 2017 Ms 7.0 Jiuzhaigou earthquake (Sichuan, China): factors controlling their spatial distribution and implications for the seismogenic blind fault identification. *Landslides* 15(5): 967-983. <https://doi.org/10.1007/s10346-018-0960-x>
- Fan XM, Scaringi G., Korup O (2019) Earthquake-induced chains of geologic hazards: patterns, mechanisms, and impacts. *Reviews of Geophysics* 57(2): 421-503. <https://doi.org/10.1029/2018RG000626>
- Fiorillo F, Guadagno FM (2012) Long karst spring discharge time series and droughts occurrence in Southern Italy. *Environmental Earth Sciences* 65(8): 2273-2283. <https://doi.org/10.1007/s12665-011-1495-9>
- Francisco LP (2001) Matrix granulometry of catastrophic debris flows (December 1999) in central coastal, Venezuela. *Catena* 45: 163-183. [https://doi.org/10.1016/S0341-8162\(01\)00149-7](https://doi.org/10.1016/S0341-8162(01)00149-7)
- Gabet EJ, Mudd SM (2006) The mobilization of debris flows from shallow landslides. *Geomorphology* 74(1-4): 207-218. <http://dx.doi.org/10.1016/j.geomorph.2005.08.013>
- Guo CB, Montgomery DR, Zhang YS, et al. (2015) Quantitative assessment of landslide susceptibility along the Xianshuihe fault zone, Tibetan Plateau, China. *Geomorphology* 248: 93-110. <https://doi.org/10.1016/j.geomorph.2015.07.012>
- Guo XJ, Cui P, Li Y et al. (2019) Evaluation of a traditional method for peak flow discharge estimation for floods in the Wenchuan Earthquake area, Sichuan Province, China. *Journal of Mountain Science* 16(3): 641-656. <https://doi.org/10.1007/s11629-018-4983-5>
- Han W, Xiong DH, Liang X, et al. (2018) Effects of vegetation coverage and seasonal change on soil microbial biomass and community structure in the dry-hot valley region. *Journal of Mountain Science* 15 (7): 1546-1558. <http://doi.org/10.1007/s11629-017-4650-2>
- Hu GS, Chen NS, Tanoli JI, et al. (2016) Case Study of the characteristics and dynamic process of July 10, 2013, catastrophic debris flows in Wenchuan County, China. *Earth Sciences Research Journal* 20 (2): E1-E13. <https://doi.org/10.15446/esrj.v20n2.48026>
- Hu KH, Cui P, Ma C, et al. (2012) Causes and characteristics of 28 June disastrous debris flow event in Ningnan County of Sichuan, China. *Journal of Mountain Science* 30 (6): 696-700. <https://doi.org/10.3969/j.issn.1008-2786.2012.06.009>
- Huang RQ, Li, WL (2014) Post-earthquake landsliding and long-term impacts in the Wenchuan earthquake area, China. *Engineering Geology* 182: 111-120. <https://doi.org/10.1016/j.enggeo.2014.07.008>
- Hürlimann M, Meardell BW, Rickli C (2015) Field and laboratory analysis of the runout characteristics of hillslope debris flows in Switzerland. *Geomorphology* 232: 20-32. <http://dx.doi.org/10.1016/j.geomorph.2014.11.030>
- Iverson RM (1997) The physics of debris flows. *Reviews of Geophysics* 35(3): 245-296. <https://doi.org/10.1029/97RG0042>
- Iverson RM (2005) Regulation of landslide motion by dilatancy and pore pressure feedback. *Journal of Geophysical Research Earth Surface* 110(F02015): 1-16. <https://doi.org/10.1029/2004JF000268>
- Jeong SW (2014) The effect of grain size on the viscosity and yield stress of fine-grained sediments. *Journal of Mountain Science* 11(1): 31-40. <http://ddoi.org/10.1007/s11629-013-2661-1>
- Kargel JS, Leonard GJ, Shugar DH, et al. (2016) Geomorphic and geologic controls of geohazards induced by Nepal's 2015 Gorkha earthquake. *Science* 351(6269): aac8353. <https://doi.org/10.1126/science.aac8353>
- Korup O (2002) Recent research on landslide dams—a literature review with special attention to New Zealand. *Progress in Physical Geography* 26(2): 206-235. <http://doi.org/10.1191/0309133302pp333ra>
- Korup O (2005) Geomorphic hazard assessment of landslide dams in South Westland, New Zealand: fundamental problems and approaches. *Geomorphology* 66(1-4): 167-188. <http://doi.org/10.1016/j.geomorph.2004.09.013>
- Larsen IJ, Montgomery DR, Korup O (2010) Landslide erosion controlled by hillslope material. *Nature Geoscience* 3(4): 247-251. <https://doi.org/10.1038/ngeo776>
- Latifi H, Prasad SN, Helweg OJ. (1994) Air entrapment and water infiltration in two-layered soil column. *Journal of Irrigation & Drainage Engineering* 120(5): 871-891. [http://doi.org/10.1061/\(ASCE\)0733-9437\(1994\)120:5\(871\)](http://doi.org/10.1061/(ASCE)0733-9437(1994)120:5(871))
- Liao M, Huang R Q, Gan J J, et al. (2013) Study of Formation Mechanism and Blocking in Giant Debris Flow at Hongchun Gully Yingxiu Town Wenchuan County. *Advanced Materials Research* 610-613: 3267-3276. <https://doi.org/10.4028/www.scientific.net/AMR.610-613.3267>
- Lin CW, Shieh CL, Yuan BD, et al. (2004) Impact of Chi-Chi earthquake on the occurrence of landslides and debris flows: example from the Chenyulan River watershed, Nantou, Taiwan. *Engineering Geology* 71(1-2): 49-61. [https://doi.org/10.1016/S0013-7952\(03\)00125-X](https://doi.org/10.1016/S0013-7952(03)00125-X)
- Liu JF, Nakatani K, Mizuyama T (2013) Effect assessment of debris flow mitigation works based on numerical simulation by using Kanako 2D. *Landslides* 10: 161-173. <https://doi.org/10.1007/s10346-012-0316-x>
- Liu JF, You Y, Chen XQ, et al., (2014) Characteristics and hazard prediction of large-scale debris flow of Xiaojia Gully in Yingxiu Town, Sichuan Province, China. *Engineering Geology* 180: 55-67. <https://doi.org/10.1016/j.enggeo.2014.03.017>
- Lu K, Yu B, Han L, et al. (2011) A study of the relationship between frequency of debris flow and the lithology in the catchment of debris flow. *Advances in Earth Science* 26(9): 980-990. (In Chinese)
- McKee TB, Doesken NJ, Kleist J (1993) The relationship of drought frequency and duration to time scales. In: 8th conference on applied climatology, Anaheim, CA. American Meteorological Society, Boston, pp. 179-184. Available online: <http://ccc.atmos.colostate.edu/relationshipofdroughtfrequency.pdf> (Accessed on 20 October 2013)
- Morris PM, Graham J, Williams DJ (1992) Cracking in drying soils. *Canadian Geotechnical Journal* 29(2): 263-277. <https://doi.org/10.1139/t92-030>
- Ni H, Zheng W, Song Z, et al. (2014) Catastrophic debris flows triggered by a 4 July 2013 rainfall in Shimian, SW China: formation mechanism, disaster characteristics and the lessons learned. *Landslides* 11(5): 909-921. <https://doi.org/10.1007/s10346-014-0514-9>
- Pareek N, Sharma ML, Arora MK. (2010) Impact of seismic factors on landslide susceptibility zonation: a case study in part of Indian Himalayas. *Landslides* 7(2): 191-201. <https://doi.org/10.1007/s10346-009-0192-1>
- Rainstorm-runoff calculation method in small watershed, Sichuan Hydrological Manual. 2010, Sichuan Water Conservancy and Power Department. Electronic publishing. Available online at: <http://www.gong123.com/kanchacehui/2012-04-30/535301.html>
- Tang C , Shi B , Liu C , et al. (2008) Influencing factors of geometrical structure of surface shrinkage cracks in clayey soils. *Engineering Geology* 101(3-4): 204-217. <https://doi.org/10.1016/j.enggeo.2008.05.005>
- Tang C, Rengers N, Van TWJ, et al. (2011) Triggering conditions and depositional characteristics of a disastrous debris flow event in Zhouqu city, Gansu Province, northwestern China.

- Natural Hazards and Earth System Science 11(11): 2903-2912.
<https://doi.org/10.5194/nhess-11-2903-2011>
- Tang C, Zhu J, Li WL, et al. (2009) Rainfall-triggered debris flows following the Wenchuan earthquake. *Bulletin of Engineering Geology and the Environment* 68(2): 187-194.
<https://doi.org/10.1007/s10064-009-0201-6>
- Theule JI, Liébault F, Loye A, et al. (2012) Sediment budget monitoring of debris-flow and bedload transport in the Manival Torrent, SE France. *Natural Hazards and Earth System Sciences* 12: 731-749.
<https://doi.org/10.5194/10.5194/nhess-12-731-2012>
- Ventisette CD, Garfagnoli F, Ciampalini A, et al. (2012) An integrated approach to the study of catastrophic debris-flows: geological hazard and human influence. *Natural Hazards & Earth System Sciences* 12(9): 2907-2922.
<https://doi.org/10.5194/nhess-12-2907-2012>
- Wei FQ, Gao KC, Hu KH, et al. (2008) Relationships between debris flows and earth surface factors in Southwest China. *Environmental Geology* 55(3): 619-627.
<https://doi.org/10.1007/s00254-007-1012-3>
- Wei W, Chen LD, Fu BJ, et al. (2010) Water erosion response to rainfall and land use in different drought-level years in a loess hilly area of China. *Catena* 81: 24-31.
<https://doi.org/10.1016/j.catena.2010.01.002>
- Wu JS, Tian LQ, Kang ZC, et al. (1993) Debris flow and its comprehensive control. Beijing: Science Press. pp 44-48. (In Chinese).
- Xu MD, Feng QH (1979) Roughness of debris flows. *Proceeding of the First Conference of Chinese Research of Debris Flows*. 51-52 (In Chinese).
- Yang ZH, Lan HX, Gao X, et al. (2015) Urgent landslide susceptibility assessment in the 2013 Lushan earthquake-impacted area, Sichuan Province, China. *Natural Hazards* 75(3): 2467-2487.
<https://doi.org/10.1007/s11069-014-1441-8>
- Yu B, Ma Y, Qi X (2013) Experimental study on the influence of clay minerals on the yield stress of debris flow. *Journal of Hydraulic Engineering* 139(4): 364-373.
[https://doi.org/10.1061/\(ASCE\)HY.1943-7900.0000679](https://doi.org/10.1061/(ASCE)HY.1943-7900.0000679)
- Yu YX, Gao MT (2001) Effects of the hanging wall and footwall on peak acceleration during the Chi-Chi Earthquake, Taiwan. *Acta seismologica sinica* 6: 615-621.
<https://doi.org/10.1007/BF02718076>
- Zhang Y, Chen NS, Liu M (2019) Debris flows originating from colluvium deposits in hollow regions during a heavy storm process in Taining, southeastern China. *Landslides*. pp 1-13.
- Zhang YZ (2004) Research on environment and discharge to Dazhai Gully and Haizi Gully debris flows in Baihetan reservoir area, Jinsha River. Chongqing, Southwest University 49 (In Chinese).
- Zhou BF, Li DJ, Luo DF (1991) Guide to prevention of debris flow. Science Press, Beijing, China (In Chinese).
- Zhou GGD, Cui P, Chen HY, et al. (2013) Experimental study on cascading landslide dam failures by upstream flows. *Landslides* 10(5): 633-643.
<https://doi.org/10.1007/s10346-012-0352-6>
- Zhou MJ, Zhou GD, Cui KFE, et al. (2019) Influence of inflow discharge and bed erodibility on outburst flood of landslide dam. *Journal of Mountain Science* 16(4): 778-792.
<https://doi.org/10.1007/s11629-018-5312-8>
- Zhou W, Tang C (2014) Rainfall thresholds for debris flow initiation in the Wenchuan earthquake-stricken area, southwestern China. *Landslides* 11(5): 877-887.
<http://doi.org/10.1007/s10346-013-0421-5>
- Zou Q, Cui P, Zeng C, et al. (2016) Dynamic process-based risk assessment of debris flow on a local scale. *Physical Geography* 37(2): 132-152.
<http://doi.org/132-152.10.1080/02723646.2016.1169477>
- Zou Q, Zhou GD, Li SS, et al. (2017) Dynamic process analysis and hazard prediction of debris flow in eastern Qinghai-Tibet Plateau area—A case study at Ridi Gully. *Arctic, Antarctic, and Alpine Research* 49(3): 373-390.
<http://doi.org/10.1657/AAAR0017-019>